

People's Democratic Republic of Algeria
Ministry of Higher Education and Scientific Research
University M'Hamed BOUGARA – Boumerdes



Institute of Electrical and Electronic Engineering
Department of Electronics

Final Year Project Report Presented in Partial Fulfilment of
the Requirements for the Degree of

‘MASTER’

In Telecommunication
Option: Telecommunications

Title:

**Design and Analysis of S-shaped
Microstrip Antenna**

Presented By:

MAMOUNE Soumia

Supervisor:

Mr. A.AZRAR

Registration Number:...../2018

Abstract

This project aimed at studying and designing S-shaped microstrip patch antenna operating at 3 GHz which is suitable for Radar application.

With a view to be familiar with microstrip antennas, this work is started by designing rectangular microstrip patch antenna working at 3 GHz. Later, the rectangular shape is modified to S-shaped antenna and it is found that it could be multiband antenna operating at 1.73 GHz (convenient for GSM application), 3 GHz (the desired radar frequency) and 4.23 GHz after small adjustments in the antenna dimensions and feed position. The obtained results show that the S-shaped antenna can operate at 1.73 GHz with size reduction of the structure of about 68%.

Both rectangular and S-shaped microstrip patch antennas are designed using transmission line model and coaxial probe feed, the simulation is done by IE3D Software.

Finally, S-shaped microstrip antenna is fabricated and tested. A good simulation and measurement results are achieved.

Dedication

I thank God, my source of knowledge and understanding for his guidance.

I dedicate my dissertation work to my family and my friends. A special feeling of gratitude to my loving parents whose words of encouragement in every step and decision I made throughout my life. Thank you both for giving me strength to chase my dreams. My brothers: Aymen, Sofiane and Fares, my sweetie sister Manel. My uncles Hafid and Ala who have supported me throughout the process and encouraged me in my many moments of crisis thanks and dedication as well.

I also dedicate this work to my friends and church family who have supported me throughout the process. I will always appreciate all they have done, especially Mebrouka for being the shoulder I can always depend on, and her continuous love, care and support.

Acknowledgment

In the name of Allah, the Most Gracious and the Most Merciful Alhamdulillah, all praises to Allah for the strengths and His blessings in completing this dissertation.

After an intensive period, today is the day: writing this note of thanks is the finishing touch on my dissertation. It has been a period of intense learning for me, not only in the scientific arena, but also on a personal level. Writing this dissertation has had a big impact on me. I would like to reflect on the people who have supported and helped me so much throughout this period.

*I would first like to thank my supervisor **Pr.Arab AZRAR**, I want to thank you for your excellent cooperation, you have been the ideal project supervisor. your sage advice, insightful criticisms, and patient encouragement aided the writing of this report in record time.*

I would like to express our sincere gratitude to Mrs. Faiza MOUHOUCHE who provided help during our work greatly needed and deeply appreciated.

Last but not least, we would like to express our gratitude to our families and friends for their love and support.

Thank You

Contents

Abstract	i
Dedication	i
Acknowledgment	ii
Introduction	1
1 Generalities	2
1.1 Microstrip Antennas	2
1.2 Feeding Techniques	4
1.2.1 Microstrip Line Feed	4
1.2.2 Coaxial Feed	5
1.2.3 Aperture Coupled Feed	5
1.2.4 Proximity Coupled Feed	6
1.3 Methods of Analysis	7
1.3.1 Transmission Line Model	7
1.3.2 Cavity Model	7
1.3.3 Full Wave Model	7
1.4 Basic Characteristics	8
1.4.1 Input Impedance	8
1.4.2 Input-Impedance Mismatch Loss	9
1.4.3 Polarization	10

1.4.4	Bandwidth	12
1.4.5	Radiation Pattern	12
1.4.6	Directivity	13
1.4.7	Antenna Radiation Efficiency	14
1.4.8	Gain	14
1.5	Microstrip Antenna Applications	15
1.6	Advantages and Disadvantages of Microstrip Antennas	16
1.6.1	Advantages	16
1.6.2	Disadvantages	16
1.7	Simulation Software IE3D	17
2	Rectangular Microstrip Patch Antenna	18
2.1	Introduction	18
2.2	Rectangular Patch Antenna Design	18
2.2.1	Rectangular Patch Width	19
2.2.2	Effective Dielectric Constant	19
2.2.3	Rectangular Patch Length	20
2.2.4	Feeding Position	21
2.3	Simulation of the Designed Antenna	21
2.3.1	Input Reflection Coefficient	22
2.3.2	Input Impedance	22
2.3.3	Voltage Standing Wave Ratio VSWR	23
2.3.4	Bandwidth	23
2.3.5	Current Distribution	23
2.3.6	Radiation Pattern	24
2.3.7	Efficiency	26
2.3.8	Radiation Resistance	26
2.4	Conclusion	27

3 S-shaped Microstrip Patch Antenna	28
3.1 Introduction	28
3.2 Design of S-shaped Microstrip Patch Antenna	28
3.2.1 Antenna Structure	28
3.3 Adjustment of the S-shaped Antenna	30
3.3.1 Final Design	30
3.3.2 Simulated Results	31
3.3.3 Efficiency	37
3.3.4 Comparison and Discussion	38
3.4 Realization and Measurements	38
3.4.1 Realization	38
3.4.2 Measurements and Comparison	39
Conclusion	41
Appendix	43

List of Figures

1.1	Microstrip Patch Antenna Configuration	2
1.2	Typical Patch Shapes	3
1.3	Fringing Fields in Rectangular Patch Antenna	4
1.4	Microstrip line feed patch antenna	5
1.5	Probe Coupling feed patch antenna	5
1.6	Aperture-Coupled feed patch antenna	6
1.7	Proximity-Coupled feed patch antenna	6
1.8	transmitting antenna and its equivalent circuit	8
1.9	Typical variation of resistance and reactance of rectangular microstrip antenna versus frequency	9
1.10	Radiation pattern in polar and cross-polar components	12
1.11	Coordinate system for antenna analysis	13
2.1	Top View of the Designed Antenna in IE3D Screen	21
2.2	Input Reflection Coefficient of Rectangular Patch Antenna.	22
2.3	Input Impedance of Rectangular Patch Antenna.	22
2.4	VSWR of Rectangular Patch Antenna	23
2.5	Current Distribution of Rectangular Patch Antenna.	24
2.6	2-D Pattern at 3 GHz and $\phi = 0^\circ$ of Rectangular Patch Antenna.	25
2.7	2-D Pattern at 3 GHz and $\phi = 90^\circ$ of Rectangular Patch Antenna.	25
2.8	3-D Pattern at 3 GHz of Rectangular Patch Antenna.	26

2.9	Radiation efficiency vs Frequency graph of Rectangular Patch Antenna.	27
3.1	The S-shaped patch antenna structure	29
3.2	Return Loss of The initial S-shaped antenna	29
3.3	Initial Current Distribution of S-shaped patch antenna	30
3.4	The S-shaped patch antenna captured from IE3D screen	31
3.5	Return Loss of S-shaped patch antenna	31
3.6	Real Part of Input Impedance of S-shaped patch antenna	32
3.7	Imaginary Part of Input Impedance of S-shaped patch antenna	33
3.8	Current Distribution of S-shaped patch antenna	34
3.9	2-D Radiation Pattern at 1.73 GHz of S-shaped patch antenna	34
3.10	2-D Radiation Pattern at 3 GHz of S-shaped patch antenna	35
3.11	2-D Radiation Pattern at 4.23 GHz of S-shaped patch antenna	35
3.12	3-D Radiation Pattern at 1.73 GHz of S-shaped patch antenna	36
3.13	3-D Radiation Pattern at 3 GHz of S-shaped patch antenna	36
3.14	3-D Radiation Pattern at 4.23 GHz of S-shaped patch antenna	37
3.15	Radiation Efficiency e_{cd} versus Frequency of S-shaped patch antenna	37
3.16	The PCB prototyping machine	38
3.17	Rear and front view of the constructed S-shaped patch antenna	39
3.18	The Vector Network Analyzer	39
3.19	Measured and Simulated Input Reflection Coefficient of S-shaped patch antenna	40
3.20	MATLAB code to plot the input reflection coefficient for both the measured and simulated results	43

List of Tables

2.1	Parameters of the dielectric substrate for the rectangular patch antenna . . .	18
2.2	Characteristics of the Rectangular Antenna	20
3.1	Dimensions of the S-shaped patch antenna	31
3.2	Reflection Coefficient and Bandwidth of the S-shaped patch antenna . . .	32
3.3	Input Impedance and VSWR of the S-shaped patch antenna	33
3.4	Maximum radiation direction, -3 dB beam-width, and maximum gain in both E-plane and H-plane at the resonant frequencies	36
3.5	Radiation efficiency, Radiation resistance at the resonant frequencies . . .	37
3.6	Measured and Simulated characteristics of S-shaped Antenna with error percentages	40

Introduction

Antennas are mandatory for a product to connect via radio frequency. Obvious examples are cell phones, satellite communications, and even our garage-door openers. But the Internet of Things is connecting less-obvious devices, such as thermostats, parking meters, wearable devices, even dog collars, and in turn bringing sweeping change to almost every industry by connecting products that previously were never connected. And it is all done wirelessly, untethered to any wire or cable [1].

Microstrip antenna was first introduced in the 1950s. However, this concept had to wait for about 20 years to be realized after the development of the printed circuit board (PCB) technology in the 1970s. Since then, microstrip antennas are the most common types of antennas with wide range of applications due to their apparent advantages of light weight, low profile, low cost, planar configuration, easy of conformal, superior portability, suitable for array with the ease of fabrication and integration with microwave monolithic integrate circuits (MMICs). They have been widely engaged for the civilian and military applications such as radio-frequency identification (RFID), broadcast radio, mobile systems, global positioning system (GPS), television, and so on [2].

Demand in communication system, in terms of speed data rate, low spectral density, high precision ranging and low cost cause the development of new antenna design. In this project the main challenge is to design S-shaped microstrip antenna reduced in size with similar performance to a rectangular patch microstrip antenna. Beginning with a general review about microstrip patch antennas and their characteristics. Then, Designing rectangular microstrip patch antenna operating at 3 GHz in the second chapter. While chapter three deals with the design of S-shaped antenna by cutting the former RMSPA to obtain more size reduction and new resonant bands. Comparison between simulated and measured result is performed as well.

Chapter 1

Generalities

1.1 Microstrip Antennas

Antenna is a transducer which transmits or receives electromagnetic waves. Microstrip antennas have several advantages over conventional microwave antenna and therefore they are used in a variety of practical applications. Microstrip antenna in its simplest design is shown in Figure 1.1. It consists of a conducting patch of any non-planar or planar geometry on one side of a dielectric substrate ($\epsilon_r \leq 10$) and a ground plane on the other side [2].

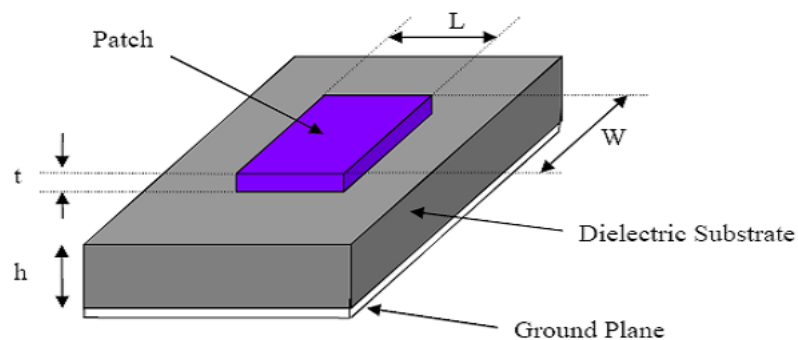


Figure 1.1: Microstrip Patch Antenna Configuration

The radiating patch may be square, rectangular, thin strip (dipole), circular, elliptical, triangular, or any other configuration. These and others are illustrated in Figure 1.2.

The rectangular and circular patches are the basic and most commonly used because of ease of analysis and fabrication, and their attractive radiation characteristics, especially low cross-polarization radiation. For a rectangular patch, the length L of the patch is usu-

ally $0.3333\lambda_0 < L < 0.5\lambda_0$, where λ_0 is the free-space wavelength. The patch is selected to be very thin such that $t \ll \lambda_0$ (where t is the patch thickness). The height h of the dielectric substrate is usually $0.003\lambda_0 \leq h \leq 0.05\lambda_0$. The dielectric constant of the substrate (ϵ_r) is typically in the range $2.2 \leq \epsilon_r \leq 12$ [3].

Thin substrates with higher dielectric constants are desirable for microwave circuitry because they require tightly bound fields to minimize undesired radiation and coupling, and lead to smaller element sizes; however, because of their greater losses, they are less efficient and have relatively smaller bandwidths [4]. Since microstrip antennas are often integrated with other microwave circuitry, a compromise has to be reached between good antenna performance and circuit design.

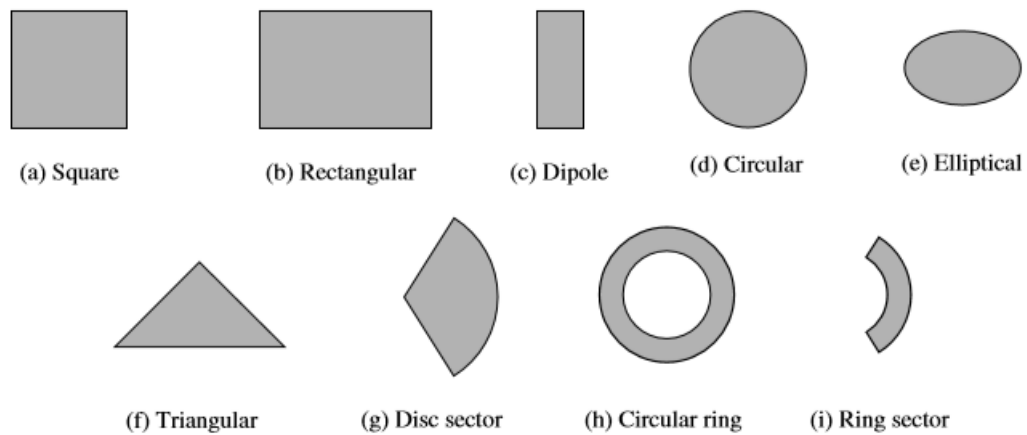


Figure 1.2: Typical Patch Shapes [4]

A patch radiates from fringing fields around its edges as illustrated in Figure 1.3. Impedance match occurs when a patch resonates as a resonant cavity. When matched, the antenna achieves peak efficiency. A normal transmission line radiates little power because the fringing fields are matched by nearby counteracting fields. Power radiates from open circuits and from discontinuities such as corners, but the amount depends on the radiation conductance load to the line relative to the patches. Without proper matching, little power radiates [5]. The edges of a patch appear as slots whose excitations depend on the internal fields of the cavity. A general analysis of an arbitrarily shaped patch considers the patch to be a resonant cavity with metal (electric) walls of the patch and the ground plane and magnetic or impedance walls around the edges. The radiating edges and fringing fields present loads along the edges [5].

Arrays of antennas can be photoetched on the substrate, along with their feeding net-

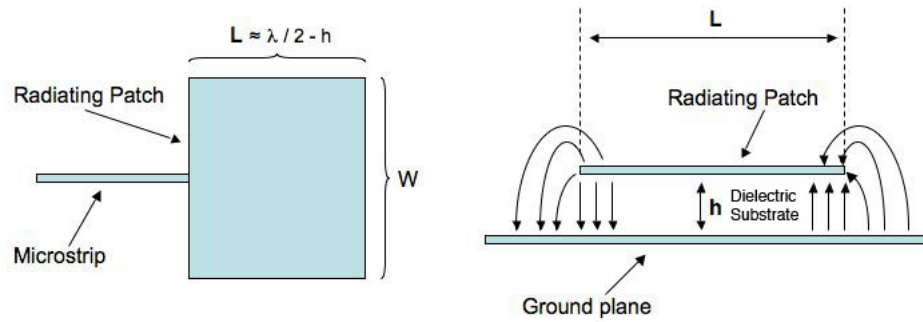


Figure 1.3: Fringing Fields in Rectangular Patch Antenna

works, and microstrip provides easy connections to active devices and allows placement of preamps or distributed transmitters next to the antenna elements. Diode phase-shifter circuits etched in the microstrip form single-board phased arrays. Microstrip circuits make a wide variety of antennas possible through the use of the simple photoetching techniques[5].

1.2 Feeding Techniques

Different methods are available to feed microstrip patch antennas. These methods can be contacting and non-contacting methods. In the contacting method, the RF power is fed directly to the radiating patch using a connecting element such as a microstrip line. In the non-contacting method, power is transferred between the microstrip line and the radiating patch through electromagnetic coupling. There are many feed techniques but the four most popular feeding techniques used are microstrip line, coaxial probe (both contacting schemes), aperture coupling and proximity coupling (both non-contacting schemes).

1.2.1 Microstrip Line Feed

In this, a conducting strip is connected directly to the edge of the microstrip patch. The conducting strip is smaller in width as compared to the patch. This kind of feed arrangement has the advantage that the feed can be etched on the same substrate to provide a planar structure [2].

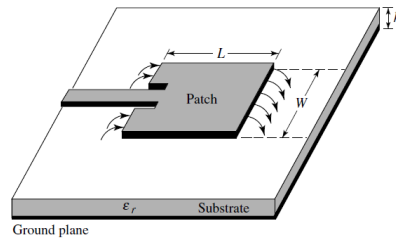


Figure 1.4: Microstrip line feed patch antenna [4]

1.2.2 Coaxial Feed

In this, the inner conductor of the coaxial connector extends throughout the dielectric and is soldered to the radiating patch, while the outer conductor is coupled to the ground plane. The major advantage of this is that the feed can be placed at any location inside the patch in order to match with its input impedance. The disadvantage is that it provides narrow bandwidth and is complex to model [2].

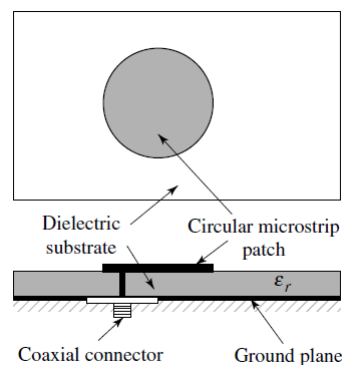


Figure 1.5: Probe Coupling feed patch antenna [4]

1.2.3 Aperture Coupled Feed

In this technique, the radiating patch and the microstrip feed line are separated by the ground plane. The patch and the feed line is coupled through a slot in the ground plane. The coupling slot is centered below the patch, leading to low cross polarization due to symmetry of the configuration. Since the ground plane separates the patch and the feed line, spurious radiation is minimized. The main disadvantage of this feed technique is that it is difficult to fabricate due to multiple layers, which also increases the antenna thickness [2].

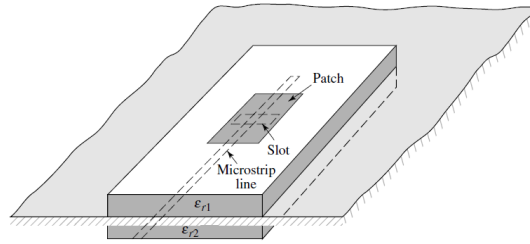


Figure 1.6: Aperture-Coupled feed patch antenna [4]

1.2.4 Proximity Coupled Feed

This type of feed technique is also called as the electromagnetic coupling scheme. Two dielectric substrates are used and the feed line is between the two substrates. The radiating patch is on top of the upper substrate. The main advantage of this feed technique is that it eliminates spurious feed radiation and provides very high bandwidth (as high as 13%). The major disadvantage of this feed scheme is that it is difficult to fabricate because of the two dielectric layers which need proper alignment [2].

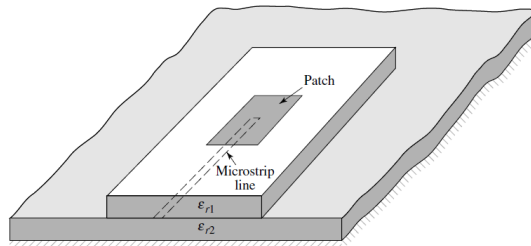


Figure 1.7: Proximity-Coupled feed patch antenna [4]

1.3 Methods of Analysis

the analysis of microstrip antenna is complicated by the presence of the dielectric inhomogeneity, inhomogeneous boundary conditions, narrow frequency band characteristics, and a wide variety of feed, patch shape, and substrate configurations. Thus there are many models for analysis and the most important are the transmission line model, cavity model, and full wave model.

1.3.1 Transmission Line Model

This model represents the microstrip antenna by two slots of width W and height h , separated by a transmission line of length L . The microstrip is essentially a non homogeneous line of two dielectrics, typically the substrate and air [4].

1.3.2 Cavity Model

In this model, the interior region of the dielectric substrate is modeled as a cavity bounded by electric walls on the top and bottom. The basis for this assumption is the following observations for thin substrates ($h \ll \lambda$). Since the substrate is thin, the fields in the interior region do not vary much in the z direction, i.e. normal to the patch. The electric field is z directed only, and the magnetic field has only the transverse components H_x and H_y in the region bounded by the patch metallization and the ground plane. This observation provides for the electric walls at the top and the bottom [4].

1.3.3 Full Wave Model

One of the methods that provide the full wave analysis for the microstrip patch antenna, is the Method of Moments. In this method, the surface currents are used to model the microstrip patch and the volume polarization currents are used to model the fields in the dielectric substrate. It has been shown by Newman and Tulyathan how an integral equation is obtained for these unknown currents. Using the Method of Moments, these electric field integral equations are converted into matrix equations, which can then be solved by various techniques of algebra to provide the result [6].

1.4 Basic Characteristics

1.4.1 Input Impedance

Input impedance is defined as the impedance presented (to the excitation circuit) by an antenna at its terminals or the ratio of the voltage to a current at a pair of terminals. In Figure 1.8, the ratio of the voltage to current at the terminals a-b defines the impedance

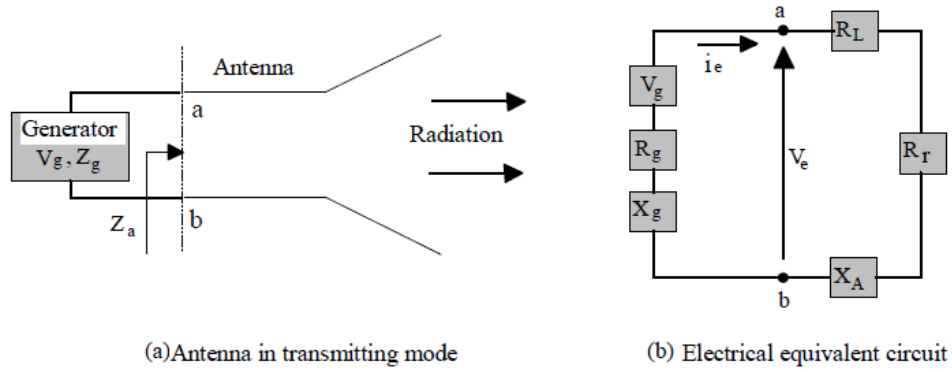


Figure 1.8: transmitting antenna and its equivalent circuit [7]

of the antenna [7].

$$Z_A = R_A + jX_A \quad (1.1)$$

The totality of power supplied to the antenna does not completely reach the receiving point. First part of it is dissipated in the antenna in the form of conductor and dielectric losses (R_L) and the second part is found as reactive power in the near zone field and it is represented by the reactive part of the input impedance. The last part, which is the objective of using antenna, is radiated to the far zones (active or radiation power, represented by R_r)[7]. The real part of the input impedance may be written as:

$$R_A = R_r + R_L \quad (1.2)$$

Where R_r is the radiation resistance of the antenna, R_L is the loss resistance of the antenna.

Both the resonant (real) and nonresonant (imaginary) parts of the impedance vary as a function of frequency, and a typical variation is shown in Figure 1.9. Ideally both the resistance and reactance exhibit symmetry about the resonant frequency, and the reactance at resonance is equal to the average of sum of its maximum value (which is positive) and its minimum value (which is negative)[4]. Typically the feed reactance is very small, compared to the resonant resistance, for very thin substrates. However, for thick elements the reactance may be significant and needs to be taken into account in impedance matching and in determining the resonant frequency of a loaded element [4].

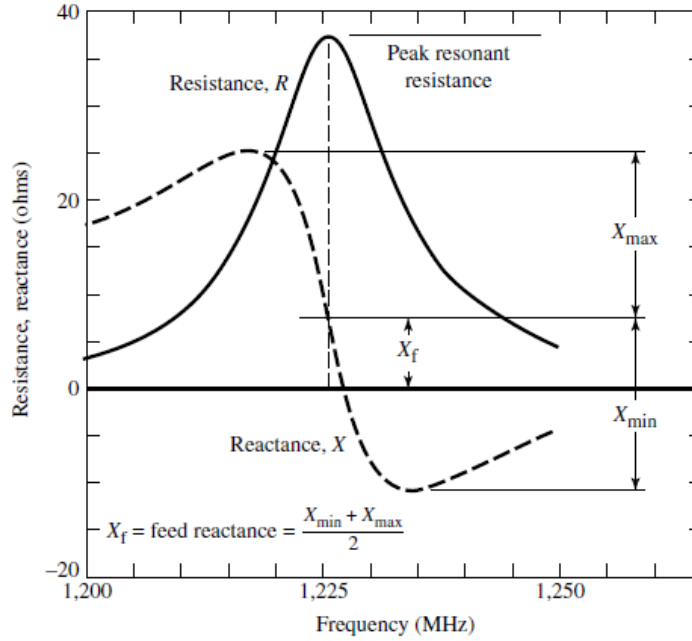


Figure 1.9: Typical variation of resistance and reactance of rectangular microstrip antenna versus frequency [4]

1.4.2 Input-Impedance Mismatch Loss

When we fail to match the impedance of an antenna to its input transmission line leading from the transmitter or to the receiver, the system degrades due to reflected power. The input impedance is measured with respect to some transmission line or source characteristic impedance. When the two are not the same, a voltage wave is reflected [5].

1.4.2.1 Return Loss

The return loss of an antenna is the most important parameter used in designing microstrip antenna is defined as the power reflected back from the antenna P_r to the source incident power of the antenna P_i . It is expressed in dB as:

$$R_L = 20 \log |\Gamma| \quad (1.3)$$

Where Γ is the reflection coefficient defined as:

$$\Gamma = \frac{Z_1 - Z_0}{Z_1 + Z_0} \quad (1.4)$$

This reflection coefficient is also equivalent to the scattering parameter S_{11} .

Z_1 is the antenna input impedance

Z_0 is the feeding line/probe characteristic impedance

1.4.2.2 VSWR

VSWR stands for Voltage Standing Wave Ratio, and is also referred to as Standing Wave Ratio (SWR). This parameter is a measure that numerically describes how well the antenna impedance is matched to the transmission line. VSWR is a function of the reflection coefficient, which describes the power reflected from the antenna, it is expressed by:

$$VSWR = \frac{1 + |\Gamma|}{1 - |\Gamma|} \quad (1.5)$$

1.4.3 Polarization

Polarization is the curve traced by the end point of the arrow (vector) representing the instantaneous electric field. The field must be observed along the direction of propagation [4]. there are three type of polarization:

1.4.3.1 Linear Polarization

A time-harmonic wave is linearly polarized at a given point in space if the electric-field vector at that point is always oriented along the same straight line at every instant of time. This is accomplished if the field vector possesses:

- a. Only one component, or
- b. Two orthogonal linear components that are in time phase or 180 (or multiples of 180) out-of-phase.

1.4.3.2 Circular Polarization

A time-harmonic wave is circularly polarized at a given point in space if the electric (or magnetic) field vector at that point traces a circle as a function of time. The necessary

and sufficient conditions to accomplish this are if the field vector (electric or magnetic) possesses all of the following:

- a. The field must have two orthogonal linear components, and
- b. The two components must have the same magnitude, and
- c. The two components must have a time-phase difference of odd multiples of 90.

1.4.3.3 Elliptical Polarization

A wave is elliptically polarized if it is not linearly or circularly polarized. Although linear and circular polarizations are special cases of elliptical, usually in practice elliptical polarization refers to other than linear or circular. The necessary and sufficient conditions to accomplish this are if the field vector (electric or magnetic) possesses all of the following:

- a. The field must have two orthogonal linear components, and
- b. The two components can be of the same or different magnitude.
- c. (1) If the two components are not of the same magnitude, the time-phase difference between the two components must not be 0 or multiples of 180 (because it will then be linear).
(2) If the two components are of the same magnitude, the time-phase difference between the two components must not be odd multiples of 90 (because it will then be circular).

1.4.3.4 Parasitic Components of Polarization

An antenna is said to have good polarization purity if the level of the cross-polarization component, noted E_{cross} , is at least -20 dB lower than the co-polar component, that polarization which the antenna is intended to radiate, noted E_{co} . The Ludwig definition of the two components of an antenna polarized along the Oy axis gives [7].

$$\begin{bmatrix} E_{co} \\ E_{cross} \end{bmatrix} = \begin{bmatrix} +\sin\phi & +\cos\phi \\ +\cos\phi & -\sin\phi \end{bmatrix} \begin{bmatrix} E_{\theta} \\ E_{\phi} \end{bmatrix}$$

If the antenna is polarized along the Ox axis, the E_{co} and E_{cross} are expressed as

$$\begin{bmatrix} E_{co} \\ E_{cross} \end{bmatrix} = \begin{bmatrix} +\cos\phi & -\sin\phi \\ +\sin\phi & +\cos\phi \end{bmatrix} \begin{bmatrix} E_{\theta} \\ E_{\phi} \end{bmatrix}$$

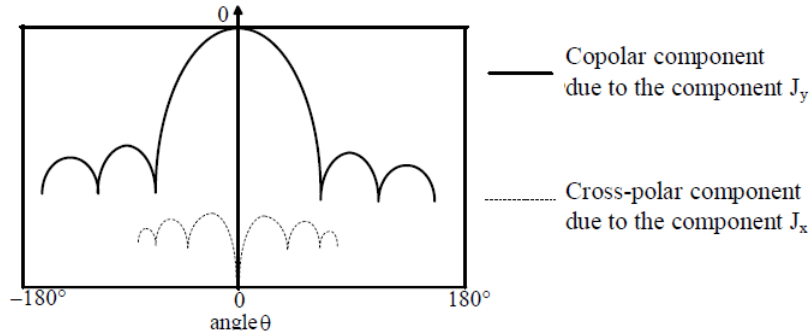


Figure 1.10: Radiation pattern in polar and cross-polar components [7]

1.4.4 Bandwidth

Bandwidth is another fundamental antenna parameter. Bandwidth describes the range of frequencies over which the antenna can properly radiate or receive energy. Often, the desired bandwidth is one of the determining parameters used to decide upon an antenna. For instance, many antenna types have very narrow bandwidths and cannot be used for wideband operation.

1.4.5 Radiation Pattern

It is important to realize that antennas radiate from currents. Design consists of controlling currents to produce the desired radiation distribution, called its pattern. The radiation pattern is defined as a mathematical function or a graphical representation of the radiation properties of the antenna as a function of space coordinates [8] as shown in Figure 1.11.

$$P_{rad} = \iint_{\Omega} U(\theta, \phi) d\Omega = \int_0^{2\pi} \int_0^{\pi} U(\theta, \phi) \sin\theta d\theta d\phi \quad (1.6)$$

where U is *radiation intensity* in a given direction is defined as "the power radiated from an antenna per unit solid angle" [9]. In mathematical form it is expressed as:

$$U(\theta, \phi) = \frac{1}{2\eta} [|E_{0\theta}|^2 + |E_{0\phi}|^2] \quad (1.7)$$

where η is the intrinsic impedance of the medium.

For a microstrip antenna, the electric field E within the patch is normal to the patch and the ground plane, and the magnetic field H is parallel to the strip edge. Polarization of a rectangular patch antenna for the dominant mode is linear and directed along the patch dimensions [8].

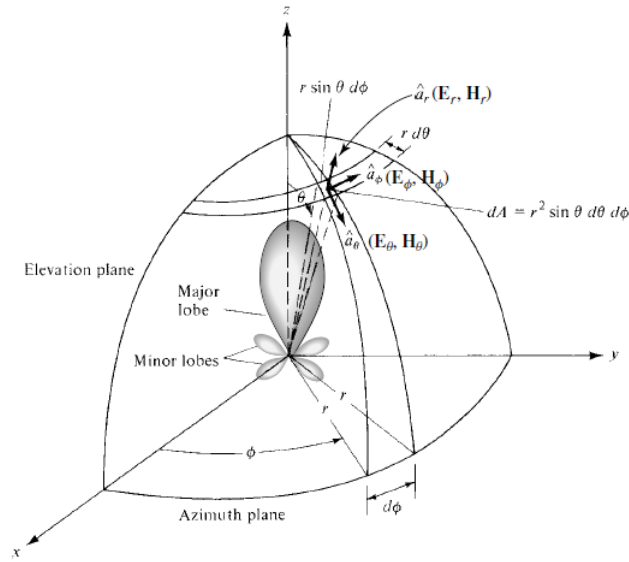


Figure 1.11: Coordinate system for antenna analysis [4]

1.4.6 Directivity

The directivity of an antenna is a measure of how much it concentrates power in a given direction, assuming the antenna is 100% efficient. The directivity of the antenna is always taken with respect to a known antenna, which is usually an isotropic radiator. On rare occasions, sometimes a half-wavelength dipole is used as a reference. Mathematically, the directivity of an antenna is defined as

$$D(\theta, \phi) = \frac{4\pi U(\theta, \phi)}{P_{rad}} \quad (1.8)$$

1.4.7 Antenna Radiation Efficiency

The antenna efficiency that takes into account the reflection, conduction, and dielectric losses. It is defined as:

$$e_0 = e_r e_c e_d \quad (1.9)$$

Where:

$e_r = 1 - |\Gamma|^2$: reflection (mismatch) efficiency.

e_c : conduction efficiency.

e_d : dielectric efficiency.

The conduction and dielectric losses of an antenna are very difficult to compute and in most cases they are measured. Even with measurements, they are difficult to separate and they are usually lumped together to form the e_{cd} efficiency. The resistance R_L is used to represent the conduction-dielectric losses.

$$e_{cd} = \frac{R_r}{R_r + R_L} \quad (1.10)$$

1.4.8 Gain

Gain is a measure of the ability of the antenna to direct the input power into radiation in a particular direction and is measured at the peak radiation intensity [6], assuming all the power supplied to the antenna is radiated (i.e., the antenna is 100% efficient). If this is not the case, then in general the input power supplied to the antenna and the radiated power from the antenna are related through [9]

$$P_{rad} = e_{cd} P_{in} \quad (1.11)$$

The term e_{cd} is the radiation efficiency of the antenna, $0 \leq e_{cd} \leq 1$. Gain is defined by replacing P_{rad} with the input power to the antenna P_{in} in equation (1.8),

$$G(\theta, \phi) = \frac{4\pi U(\theta, \phi)}{P_{in}} = e_{cd} \frac{4\pi U(\theta, \phi)}{P_{rad}}$$

$$G(\theta, \phi) = e_{cd} D(\theta, \phi) \quad (1.12)$$

1.5 Microstrip Antenna Applications

The usage of the microstrip antennas is spreading widely in all the fields and areas and now they are booming in the commercial aspects due to their low cost of the substrate material and the fabrication. Some of the applications are:

- Radar application.
- Mobile satellite communication system
- Direct broadcast television
- Wireless LAN's
- Feed Elements in coaxial system
- Global Positioning Systems (GPS).
- Missiles and telemetry
- UHF patch antenna for space
- Radio frequency identification (RFID).
- Worldwide Interoperability for Microwave Access (WiMax).
- Telemedicine application.

1.6 Advantages and Disadvantages of Microstrip Antennas

1.6.1 Advantages

- They operate at microwave frequencies where traditional antennas are not feasible to be designed.
- This antenna type has smaller size and hence will provide small size end devices.

- The microstrip based antennas are easily etched on any PCB and will also provide easy access for troubleshooting during design and development. This is due to the fact that microstrip pattern is visible and accessible from top. Hence they are easy to fabricate and comfortable on curved parts of the device. Hence it is easy to integrate them with MICs or MMICs.
- As the patch antennas are fed along centerline to symmetry, it minimizes excitation of other undesired modes.
- The microstrip patches of various shapes e.g. rectangular, square, triangular etc. are easily etched.
- They have lower fabrication cost and hence they can be mass manufactured.
- They are capable of supporting multiple frequency bands (dual, triple).
- They support dual polarization types linear and circular both.
- They are light in weight.
- They are robust when mounted on rigid surfaces of the devices.

1.6.2 Disadvantages

- The spurious radiation exists in various microstrip based antennas such as microstrip patch antenna, microstrip slot antenna and printed dipole antenna.
- It offers low efficiency due to dielectric losses and conductor losses.
- It offers lower gain.
- It has higher level of cross polarization radiation.
- It has lower power handling capability.
- It has inherently lower impedance bandwidth.
- The microstrip antenna structure radiates from feeds and other junction points.

1.7 Simulation Software IE3D

IE3D is the first SCALABLE EM design and verification platform that delivers the modeling accuracy for the combined needs of high-frequency circuit design and signal integrity engineers across multiple design domains. IE3D's multi-threaded and distributed simulation architecture and high-design capacity is the most cost-effective EM simulation and modeling solution for component-level and circuit-level applications [10]. It has been widely used in the design of MICs, RFICs, patch antennas, wire antennas, and other RF/Wireless antennas. It can be used to calculate and plot the S-parameters, VSWR, current distributions as well as the radiation patterns. Some of IE3D's features are:

- High efficiency, high accuracy, low cost electromagnetic simulation tool on PCs with windows based graphic interface and efficient matrix solvers
- Automatic generation of non-uniform mesh with rectangular and triangular cells.
- Can model structure with finite ground planes and differential feed structures.
- Accurate modelling of true 3D metallic structures and metal thickness. 3D and 2D display for current distribution, radiation patterns and near field.

Chapter 2

Rectangular Microstrip Patch Antenna

2.1 Introduction

In the previous chapter, microstrip patch antennas have been discussed in general. In this chapter, a rectangular shaped microstrip patch antenna will be studied and designed to operate at 3 GHz using transmission line model. The antenna excited with coaxial probe feed and the simulation process had done by IE3D simulator software.

2.2 Rectangular Patch Antenna Design

The microstrip patch has been designed for 3 GHz operation using the FR4 epoxy glass as dielectric substrate which has the following parameters :

Table 2.1: Parameters of the dielectric substrate for the rectangular patch antenna

dielectric Substrate	Thickness (h)	Tangent loss ($\tan \delta$)	Relative permittivity (ϵ_r)
	1.62 mm	0.018	4.3

Where:

- h is the height of the substrate.
- ϵ_r is the dielectric constant of the substrate.
- $\tan \delta$ is the tangent loss of the substrate.

The design flow for the rectangular patch dimensions, using the transmission line model approach is as follows:

The first approximation we make is to assume that the thickness of the conductor t that forms the line has no effect on our calculations, because it is very thin comparing with the substrate h , ($h \gg t$); so we use here empirical formulas that depend only on the line dimensions: The width W , the length L , the height h , and the dielectric constant ϵ_r of the substrate [8].

2.2.1 Rectangular Patch Width

The width of the microstrip line is given by:

$$W = \frac{c}{2f_r} \sqrt{\frac{2}{\epsilon_r + 1}} \quad (2.1)$$

with $c = 3 \times 10^8 \text{ m/s}$, $f_r = 3 \text{ GHz}$, $\epsilon_r = 4.3$ results in

$$W = 30.71 \text{ mm}$$

2.2.2 Effective Dielectric Constant

The effective dielectric constant ϵ_{reff} can be defined as: "the dielectric constant of the uniform dielectric material so that the air around the patch and the dielectric material of the substrate have identical electrical characteristics, particularly propagation constant". This will lead to $1 < \epsilon_{reff} < \epsilon_r$. For $\epsilon_r \ll 1$, ϵ_{reff} is closer to the actual value of the dielectric constant ϵ_r of the substrate.

The effective dielectric constant ϵ_{reff} can be calculated from the formula:

$$\epsilon_{reff} = \left(\frac{\epsilon_r + 1}{2}\right) + \left(\frac{\epsilon_r - 1}{2}\right) \frac{1}{\sqrt{1 + \frac{12h}{W}}} \quad (2.2)$$

Using values in Table 2.1 yields:

$$\epsilon_{reff} = 3.94$$

2.2.3 Rectangular Patch Length

The microstrip patch antenna in figure 1.3 looks longer than its physical dimensions because of the effect of fringing. The effective length therefore is differing from the physical length by $2\Delta L$. Then, the actual length is [5]:

$$L = L_{eff} - 2\Delta L \quad (2.3)$$

A very popular approximation to calculate the extension of the length of the patch is given by [8]:

$$\Delta L = 0.412h \frac{(\epsilon_{reff} + 0.3)\left(\frac{W}{h} + 0.264\right)}{(\epsilon_{reff} - 0.258)\left(\frac{W}{h} + 0.8\right)} \quad (2.4)$$

$$\Delta L = 0.74mm$$

and the effective length is defined by [4]:

$$L_{eff} = \frac{c}{2f_r \sqrt{\epsilon_{reff}}} \quad (2.5)$$

By substituting:

$$\mathbf{L = 23.70 mm}$$

A slight adjustment consisting on the antenna length decrease has been performed to achieve the desired resonant frequency. Thus, according to the used simulator the antenna length yielding the desired resonant frequency is **L = 22.775 mm**.

The complete characteristics of the designed antenna are summarized in the following Table 2.2.

Table 2.2: Characteristics of the Rectangular Antenna

Operating frequency f_r	Substrate thickness h	Dielectric constant ϵ_r	Patch Length L	Patch Width W
3 GHz	1.62 mm	4.3	22.775 mm	30.71 mm

2.2.4 Feeding Position

There are many configurations that can be used to feed microstrip antennas. The four most popular feeding are the microstrip line, coaxial feed, aperture coupling and proximity coupling, as it is mentioned in the previous chapter. The feeding technique which is used in this project is coaxial probe feeding.

To optimize the antenna efficiency for transmitting and receiving the patch impedance should match with the feed. The patch impedance depends on the feed position; hence it becomes very necessary to optimize the feed position.

2.3 Simulation of the Designed Antenna

Using the IE3D simulator, and after entering the specific parameters we have drawn the rectangular patch antenna shown in Figure 2.1.

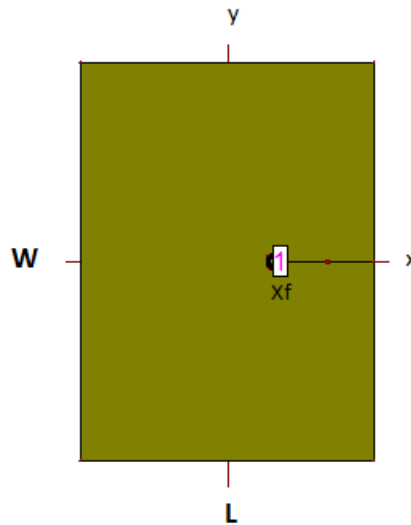


Figure 2.1: Top View of the Designed Antenna in IE3D Screen

Several iterations are carried out by varying X_f for estimating the feed point coordinates that leads to matching. It could be clearly noticed that, the nearer the feeding point from the center, the lower the input resistance. The optimal position that results in impedance real part of 50Ω and null reactance is **(3.87 mm, 0)**.

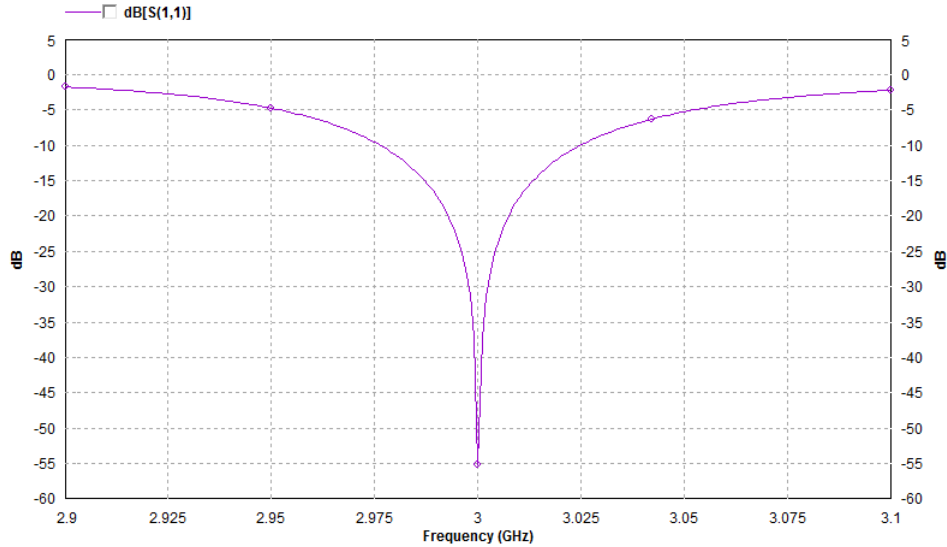


Figure 2.2: Input Reflection Coefficient of Rectangular Patch Antenna.

2.3.1 Input Reflection Coefficient

After simulating the structure, the obtained reflection coefficient (return loss) is shown in Figure 2.2. It is clear that the antenna is resonating at the desired frequency, 3 GHz, where the magnitude of the input reflection coefficient is about -55 dB (45 dB lower than -10 dB).

2.3.2 Input Impedance

The input impedance versus frequency is plotted in Figure 2.3. The figure shows clearly that the real part at $f = 3\text{GHz}$ is 50Ω and the imaginary part is almost zero.

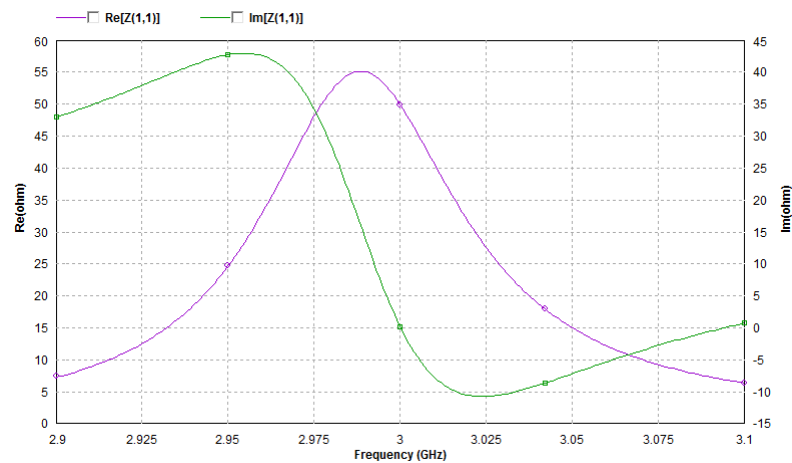


Figure 2.3: Input Impedance of Rectangular Patch Antenna.

2.3.3 Voltage Standing Wave Ratio VSWR

Also the VSWR was recorded and as shown in Figure 2.4 at $f = 3\text{GHz}$, $VSWR = 1.0035$. All the obtained results affirm that the feed position was the optimum choice.

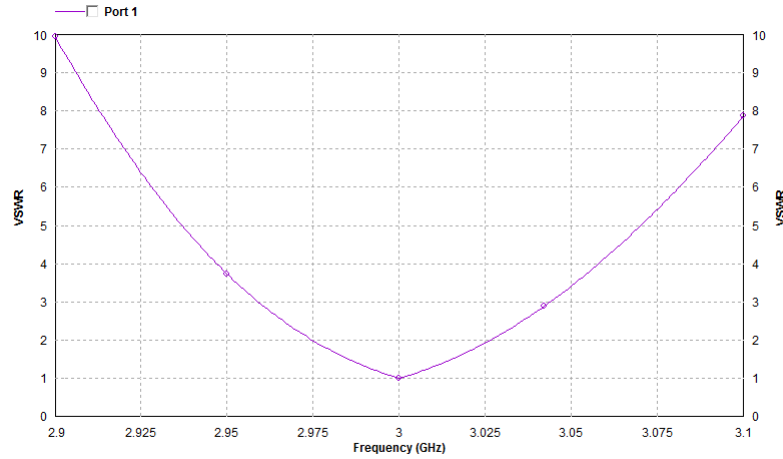


Figure 2.4: VSWR of Rectangular Patch Antenna .

2.3.4 Bandwidth

The bandwidth of the antenna is the range of frequencies within which the performance of the antenna, with respect to some characteristics, conforms to a specified standard. It can be calculated using the graph of the input reflection coefficient evaluated to -10 dB or the graph of VSWR evaluated to 2, calculation result given below, shows that the structure has narrow bandwidth.

$$BW = \frac{3.024 - 2.976}{3} \times 100 = 1.6\%$$

2.3.5 Current Distribution

Figure 2.5 , shows the current distribution of the patch at 3 GHz, the current is minimum near the left and right edges and maximum between them. Thus, the patch acts as half wavelength dipole antenna which illustrates the role of re-sizing the length in order to adjust the resonance frequency.

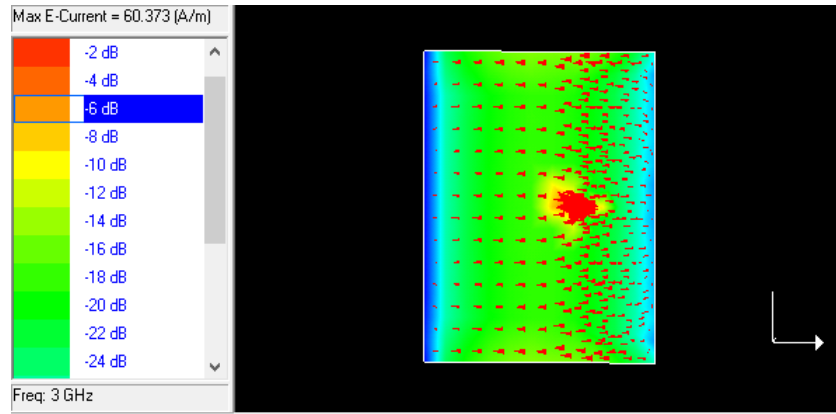


Figure 2.5: Current Distribution of Rectangular Patch Antenna.

2.3.6 Radiation Pattern

2.3.6.1 2-D Pattern

The 2-D representation of the far field patterns where the angular field distribution is essentially independent of the distance from a specified point in the antenna region, are shown in Figures 2.6 and 2.7. It is evident that the maximum radiation is perpendicular to the ground plane of the antenna ($\theta = 0^\circ$), with gain of **5.464 dBi**.

Since the excitation point is on the x-axis, the antenna is x-polarized (polarized along the x-axis). The corresponding parasitic components are given as:

$$\begin{bmatrix} E_{co} \\ E_{cross} \end{bmatrix} = \begin{bmatrix} +\cos\phi & -\sin\phi \\ +\sin\phi & +\cos\phi \end{bmatrix} \begin{bmatrix} E_\theta \\ E_\phi \end{bmatrix}$$

For $\phi = 0^\circ$ (E-plane):

$$E_{co} = E_\theta$$

$$E_{cross} = E_\phi$$

For $\phi = 90^\circ$ (H-plane):

$$E_{co} = E_\phi$$

$$E_{cross} = E_\theta$$

To study the polarization purity, both co-polar and cross-polar components of the radiated field are drawn in the E-plane and H-plane,

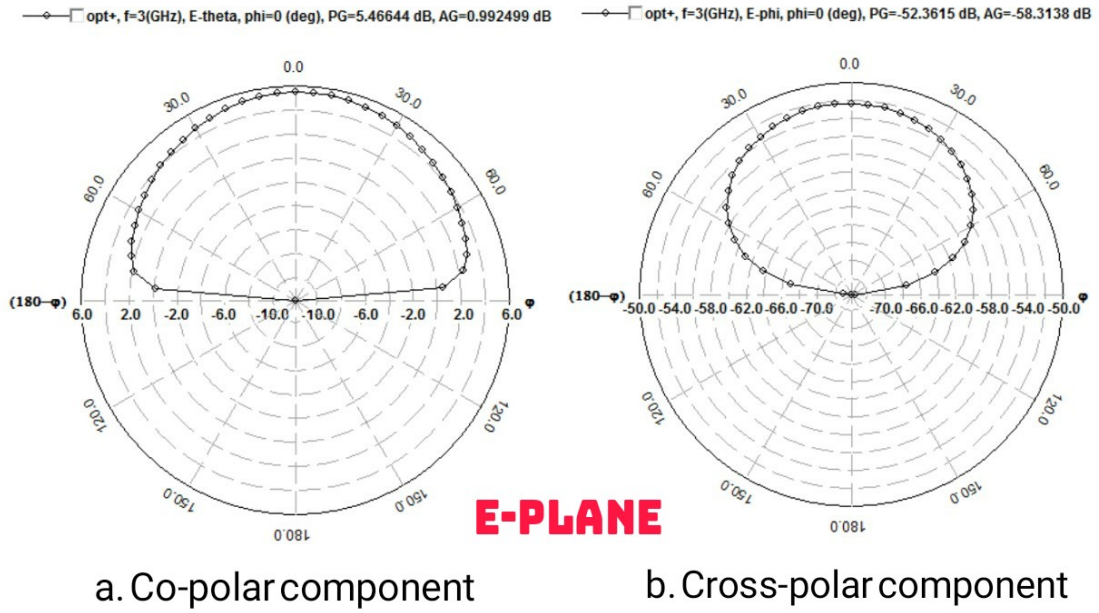


Figure 2.6: 2-D Pattern at 3 GHz and $\phi = 0^\circ$ of Rectangular Patch Antenna.

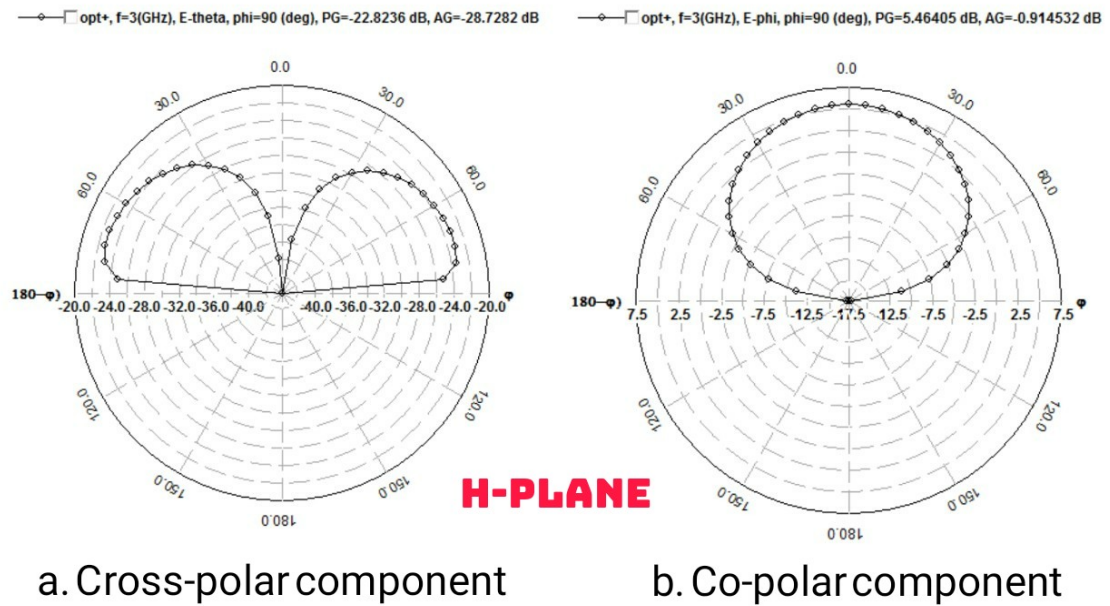


Figure 2.7: 2-D Pattern at 3 GHz and $\phi = 90^\circ$ of Rectangular Patch Antenna.

Based on the recorded values at $\theta = 0^\circ$ of the co-polar and the cross-polar components in E-plane, the cross-polar component is **57.82 dB** lower than the co-polar component. Then the antenna has a good purity of polarization.

2.3.6.2 3-D Pattern

The obtained 3D radiation pattern after simulation at the resonant frequency is shown in Figure 2.8. It is the pattern in the actual 3D space. The size of the pattern from the origin represents how strong the field at a specific (θ, ϕ) angle.

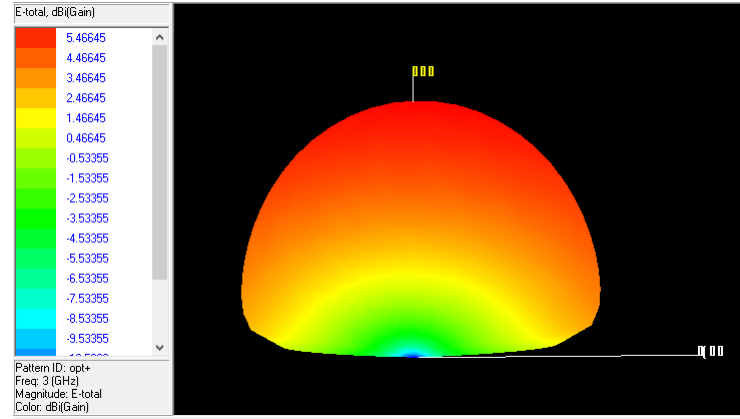


Figure 2.8: 3-D Pattern at 3 GHz of Rectengular Patch Antenna.

2.3.7 Efficiency

The radiation efficiency e_{cd} is calculated using equation (1.12) and the 2D radiation pattern of E-plane. At the maximum radiation direction ($\theta = 0^\circ$):

$$G(dBi) = e_{cd}(dBi) + D(dBi)$$

$$e_{cd} = -1.047dBi = \mathbf{78.57\%}$$

Otherwise, the radiation efficiency could be recorded directly using IE3D simulator from Efficiency versus Frequency graph option as followed:

From the graph Radiation Efficiency = **78.57%** which is good.

2.3.8 Radiation Resistance

Since the radiation efficiency and the input impedance are known, the radiation resistance can be calculated by equation (1.11):

$$e_{cd} = \frac{R_r}{R_r + R_L}$$

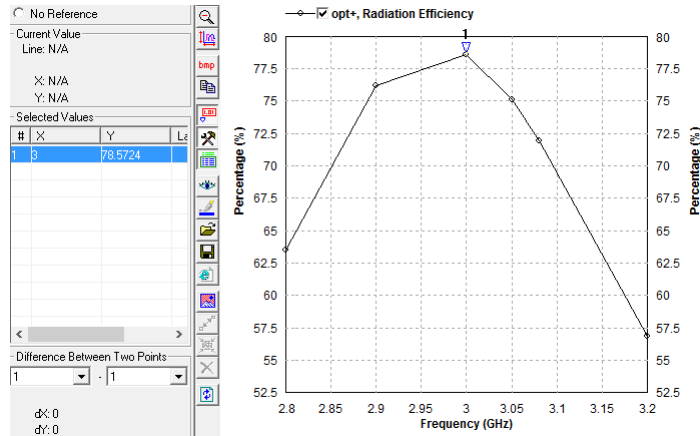


Figure 2.9: Radiation efficiency vs Frequency graph of Rectangular Patch Antenna.

knowing that the real part of input impedance is:

$$R_{in} = R_r + R_L = 50\Omega$$

Then,

$$R_r = 39.28\Omega$$

2.4 Conclusion

In this chapter, a rectangular microstrip patch antenna is designed. Transmission line model is used to get the approximate size of the antenna to which a slight adjustment has been performed using the IE3D software to achieve the desired resonant frequency with an operating frequency of 3 GHz. A trial and error method is used to locate the feed point position.

The designed rectangular microstrip patch antenna efficiently resonates at 3GHz and gives good return loss of -55 dB with an impedance matching of 50Ω , directivity of 6.51 dBi. While, the radiation efficiency comes out to be 78.57%.

Chapter 3

S-shaped Microstrip Patch Antenna

3.1 Introduction

When it comes to these modern connected devices, the antenna size reduction is very important for industrial designers and device manufacturers, since the selection of the antennas depends on the application, the available board size, cost, RF range, and directivity [6]. For these reasons, many researches had done and many arbitrary designs have been proposed to achieve those qualifications.

This dissertation aimed to design S-shaped microstrip antenna with the same performance of the rectangular one. In this chapter, using the rectangular patch antenna which is designed in the previous chapter, S-shaped multiband antenna is obtained by cutting two slots from the rectangle. Then, focusing on 3 GHz (RADAR application) and 1.75 GHz (GSM application) bands, since they are the most commercially used, several adjustments in the antenna dimensions have done to achieve an optimum matching.

3.2 Design of S-shaped Microstrip Patch Antenna

3.2.1 Antenna Structure

This section introduces the design of our antenna. In order to design the S-shaped antenna, two rectangular slots are subtracted from the designed rectangular patch in the previous chapter, as illustrated in Figure 3.1. The initial slot's dimensions are: $l = 8 \text{ mm}$, $m = 5$

$mm, k = 5 mm$.

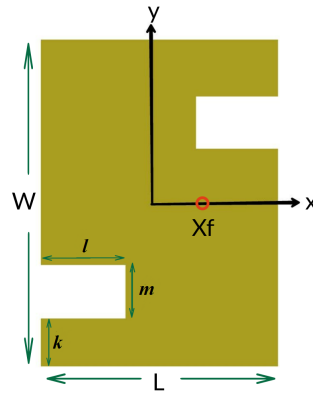


Figure 3.1: The S-shaped patch antenna structure

Using the same probe feed position ($3.87mm, 0$) with the same characteristics, the simulated input reflection coefficient (S_{11}) is shown in Figure 3.2.

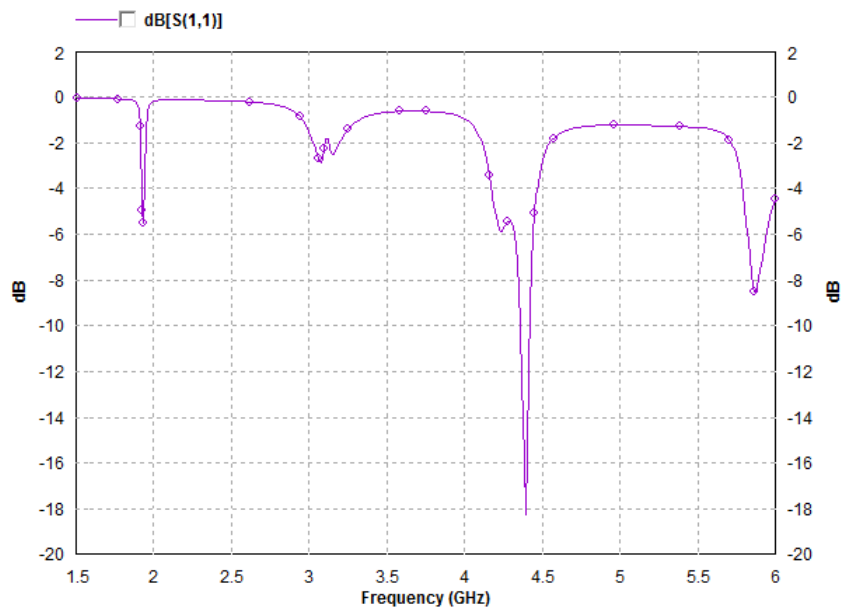


Figure 3.2: Return Loss of The initial S-shaped antenna

From Figure 3.2, it is clear that there is no resonance at 3 GHz but there are two new resonant frequencies obtained at **1.93 GHz** and **4.33 GHz**. In the next section, the design would be adjusted to recover the original frequency 3 GHz and optimize the other frequencies.

3.3 Adjustment of the S-shaped Antenna

The aim of this section is to make the S-shaped microstrip patch antenna resonates at the most commercially used frequencies 3 GHz which is used in radar application, and 1.73 GHz that is used for GSM applications [4]. In order to estimate which parameter could be adjusted to end up with resonance at those frequencies, the current distribution at each frequency is displayed by the simulator and shown in the Figure 3.3.

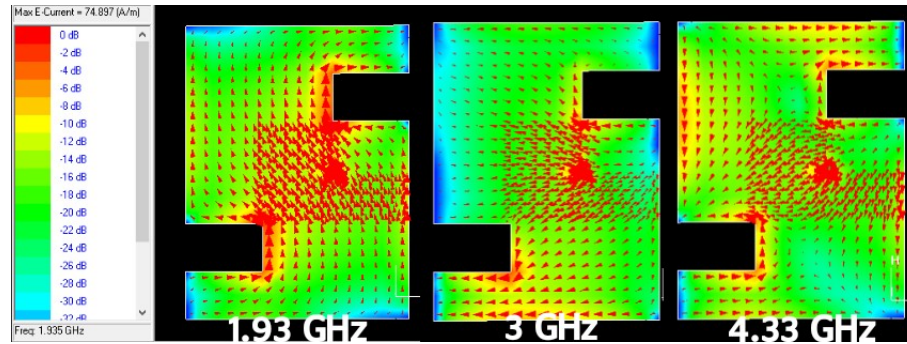


Figure 3.3: Initial Current Distribution of S-shaped patch antenna

At 1.93 GHz, the current is zero at the corners and it has vertical direction from the bottom zero to the top one. Thus, it is supposed that the resonant length that controls the resonant frequency is $L' = l + m + l + (W - m - k)$. Since the wavelength of the antenna at 1.93 GHz is 82.99 mm which is approximately twice the resonant length ($L' = 41.71\text{mm}$), then the estimation is correct. At the 3 GHz the current kept the same distribution as in the rectangular shape and the resonant length is L as in the previous chapter. Whereas at 4.33 GHz, the current has six zeros and it is supposed to be the second mode of the first frequency (1.93 GHz).

3.3.1 Final Design

With a view to achieve resonance at 1.73 GHz and 3 GHz, l is increased to **10.48 mm**, which means that the resonant length for 1.93 GHz is increased. Furthermore, L is increased to **23.30 mm** with probe feed at (**3.85 mm, 0 mm**). The updated antenna dimensions are summarized in Table 3.1 and the final shape is shown in Figure 3.4 .

Table 3.1: Dimensions of the S-shaped patch antenna

W (mm)	L (mm)	l (mm)	m (mm)	k (mm)	Feed Position(mm)
30.71	23.30	10.48	5	5	(3.85, 0)

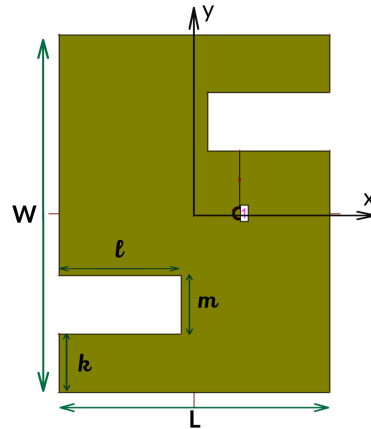


Figure 3.4: The S-shaped patch antenna captured from IE3D screen

3.3.2 Simulated Results

3.3.2.1 Return Loss

After several trials, the optimum return loss that could be acquired is shown in Figure 3.5 with antenna dimensions mentioned in Table 3.1.

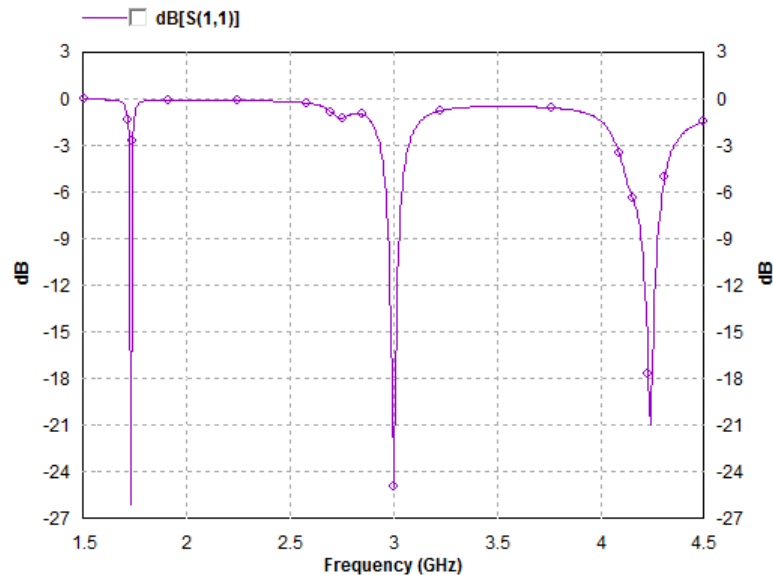


Figure 3.5: Return Loss of S-shaped patch antenna

The figure illustrates clearly that the desired resonant frequencies 3 GHz and 1.73 GHz are attained with reflection coefficients lower than -10 dB and the corresponding

bandwidths at each frequency are mentioned in Table 3.2. There are other modes of the original resonant frequencies (1.73 GHz and 3 GHz) after 4.5 GHz which are matched but they are not the interest of this project.

Table 3.2: Reflection Coefficient and Bandwidth of the S-shaped patch antenna

Frequency	Return Loss (S_{11})	Bandwidth
1.73 GHz	-26.11 dB	0.35%
3.00 GHz	-24.96 dB	1.47%
4.23 GHz	-20.91 dB	1.65%

3.3.2.2 Input Impedance

As known, impedance matching is one of the most challenging factors, as it is required to have a voltage standing wave ratio $VSWR < 2$, reduce the size and also match the impedance to 50Ω at resonant frequencies. The input impedance of the antenna around the three resonant frequencies (1.73 GHz, 3 GHz and 4.23 GHz) is plotted in Figures 3.6 and 3.7, and Table 3.3 shows the corresponding values.

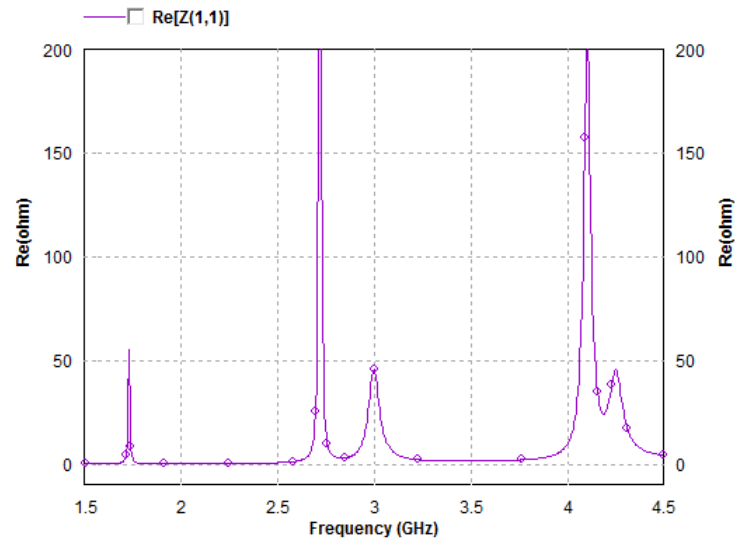


Figure 3.6: Real Part of Input Impedance of S-shaped patch antenna

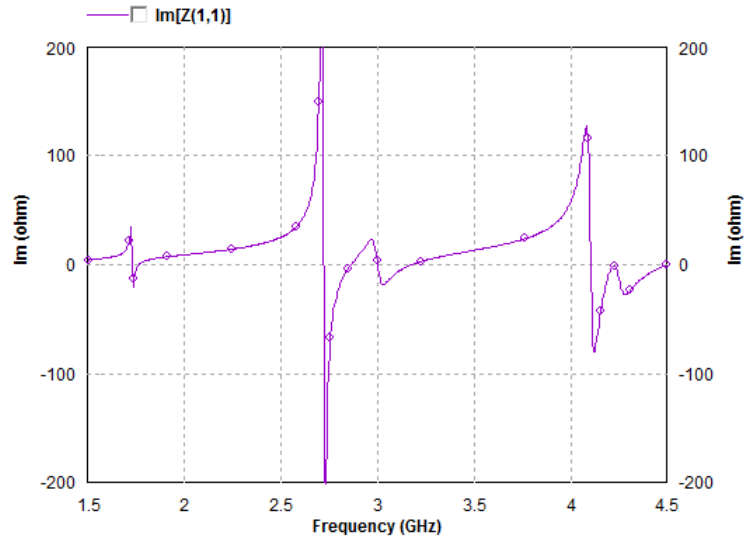


Figure 3.7: Imaginary Part of Input Impedance of S-shaped patch antenna

Table 3.3: Input Impedance and VSWR of the S-shaped patch antenna

Frequency	Real Part of Z_{in}	Imaginary Part of Z_{in}	VSWR
1.73 GHz	55.07Ω	-0.50Ω	1.12
3.00 GHz	45.68Ω	3.25Ω	1.11
4.23 GHz	43.25Ω	-5.01Ω	1.19

The antenna is well matched to the coaxial probe feed, these values affirm the judicious choice of the feed point position. However, the two plots show that there is resonance at 2.72 GHz and 4.08 GHz. They did not appear in the reflection coefficient graph because of the impedance mismatch, but they can be matched by adjusting the feeding position. Since they are not the concern of this work, so they are ignored.

3.3.2.3 Current Distribution

The current distribution of the patch is drawn (in Figure 3.8) at the three resonant frequencies 1.73 GHz, 3 GHz and 4.23 GHz. At the first two frequencies the patch is similar to half wavelength dipole and the last frequency represents the second mode of 1.73 GHz frequency; as it is mentioned at the beginning of this section. The polarization at the first frequency is a little bit tilted.

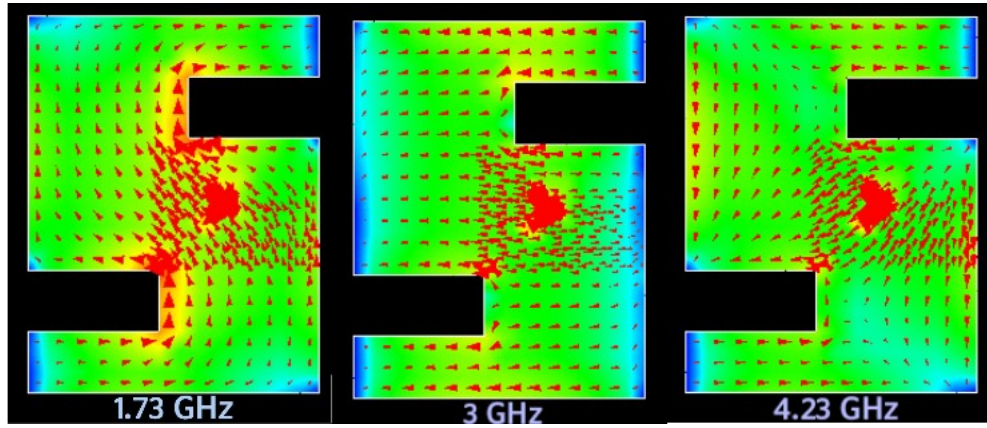


Figure 3.8: Current Distribution of S-shaped patch antenna

3.3.2.4 Radiation Pattern

The antenna 2-D representation of the far zone radiation patterns at the resonant frequencies in E-plane and H-plane are plotted in Figures 3.9, 3.10 and 3.11 .

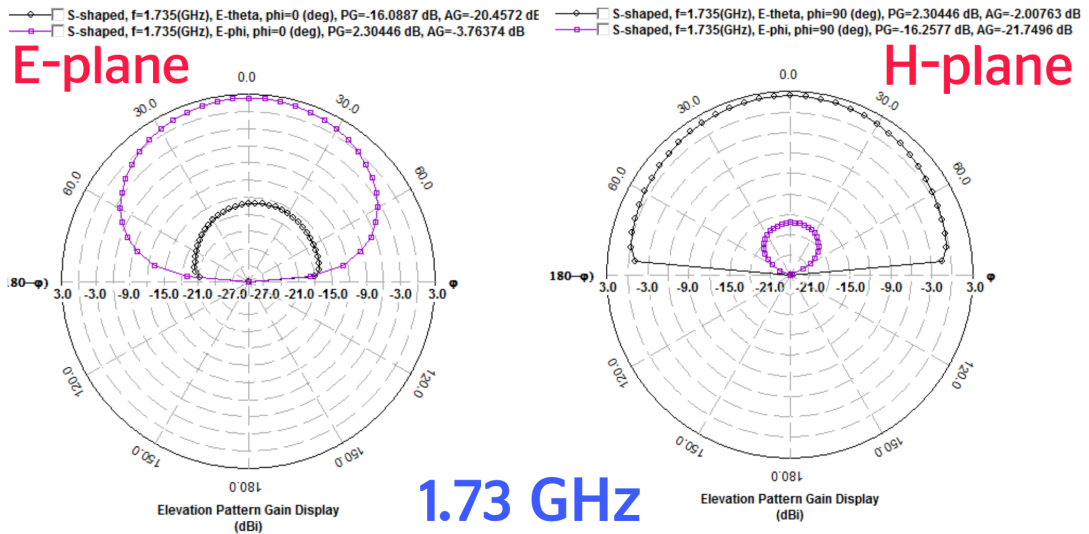


Figure 3.9: 2-D Radiation Pattern at 1.73 GHz of S-shaped patch antenna

At 1.73 GHz,

- In E-plane ($\phi = 0$):

$$E_{\theta} \approx 0 \Rightarrow E_{\theta} = E_{cross}$$

$$E_{\phi} > 0 \Rightarrow E_{\phi} = E_{co}$$

- In H-plane ($\phi = \frac{\pi}{2}$):

$$E_{\theta} > 0 \Rightarrow E_{\theta} = E_{co}$$

$$E_{\phi} \approx 0 \Rightarrow E_{\phi} = E_{cross}$$

Based on Ludwig definition (Chapter 1) and the obtained figure it can be seen that the antenna at 1.73 GHz is polarized along **y-axis** with a level of cross-polarized component of about -18 dB below the copolar component in the maximum radiation direction.

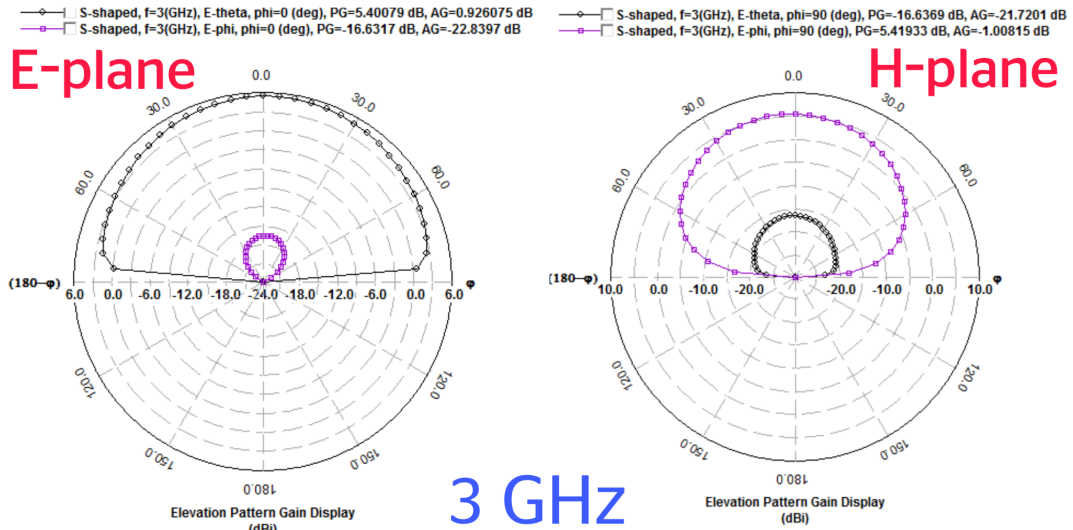


Figure 3.10: 2-D Radiation Pattern at 3 GHz of S-shaped patch antenna

The antenna at 3 GHz has the same polarization as in rectangular shape which is along **x-axis** and the level of the cross-polarized component is about -20 dB below the copolar component in the maximum radiation direction.

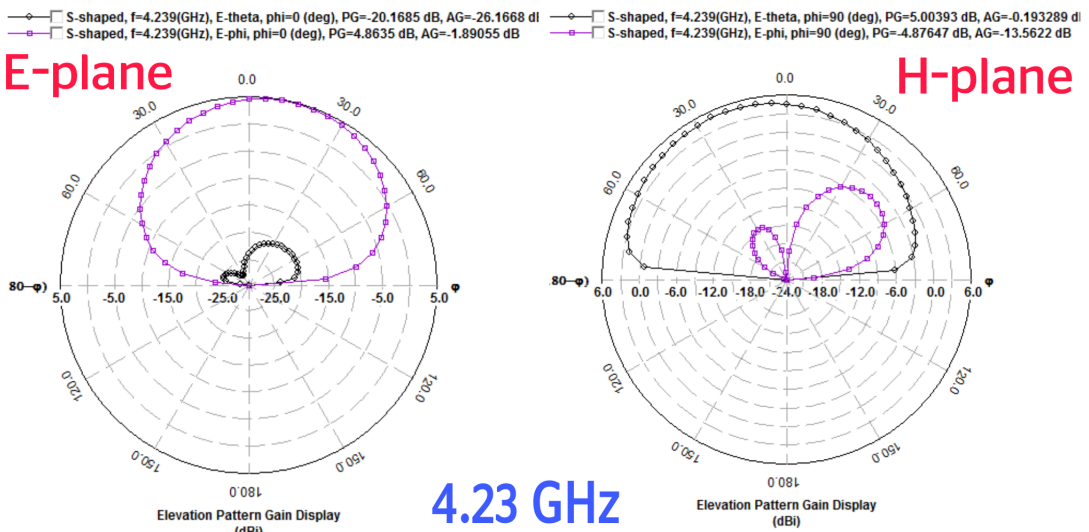


Figure 3.11: 2-D Radiation Pattern at 4.23 GHz of S-shaped patch antenna

Figure 3.11 indicates clearly that the patterns correspond to a mode. The maximum

radiation direction is no more in the broadside ($\theta = 0^\circ$) and the drawing of the total field (not shown here) shows secondary lobes. The polarization at 4.23 GHz is off main axes.

The values of the maximum radiation directions, -3 dB beamwidths and maximum gain corresponding to each frequency are summarized in Table 3.4 for both E-plane and H-plane.

Table 3.4: Maximum radiation direction, -3 dB beam-width, and maximum gain in both E-plane and H-plane at the resonant frequencies

Frequency GHz	E-plane			H-plane		
	maximum gain	max direction	-3dB Beamwidth	maximum gain	max direction	-3dB Beamwidth
1.73	1.12 dB	0°	102°	1.12 dB	0°	170°
3.00	5.42 dB	0°	170°	5.44 dB	-4.94°	127°
4.23	4.59 dB	14.88°	112°	4.85 dB	-24.89°	162°

To have a global picture on the radiation of this antenna, the simulated 3D radiation patterns at the resonant frequencies are plotted in Figures 3.12, 3.13 and 3.14 . The radiation pattern is similar to a dipole pattern, at the first and second resonant frequencies. While at the third, the pattern looks like a slightly pinched dipole pattern

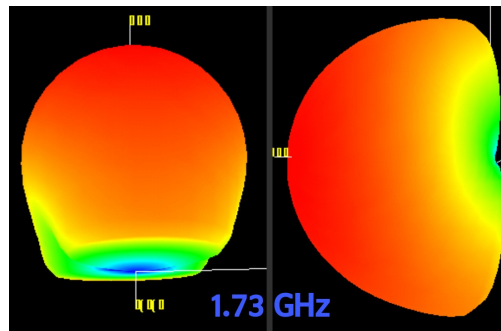


Figure 3.12: 3-D Radiation Pattern at 1.73 GHz of S-shaped patch antenna

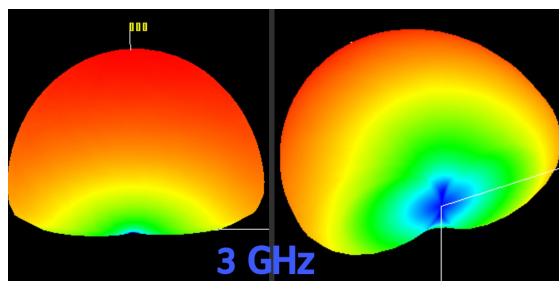


Figure 3.13: 3-D Radiation Pattern at 3 GHz of S-shaped patch antenna

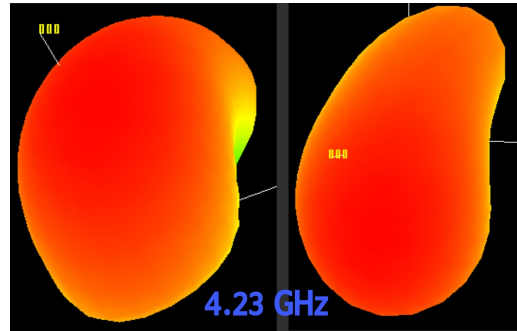


Figure 3.14: 3-D Radiation Pattern at 4.23 GHz of S-shaped patch antenna

3.3.3 Efficiency

The radiation efficiency versus frequency is plotted in Figure 3.15 . Then the radiation resistance is calculated at each frequency by Equation 1.4, the results are listed in Table 3.5. From the obtained results, the radiation efficiency and resistance increase with frequency as expected. However, a decrease of these parameters is noticed by moving from the second to the third frequency. This is explained by the fact that when operating at the third frequency the first mode is also excited and the delivered power will be spread between the two modes leading to degradation of the radiation efficiency at the second mode frequency.

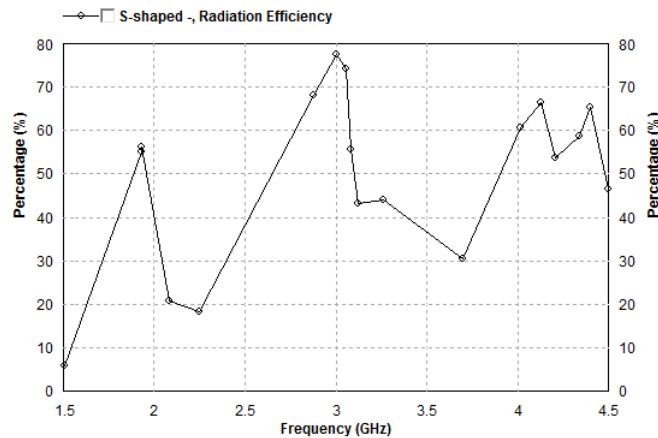


Figure 3.15: Radiation Efficiency e_{cd} versus Frequency of S-shaped patch antenna

Table 3.5: Radiation efficiency, Radiation resistance at the resonant frequencies

Frequency	Radiation efficiency e_{cd}	Radiation resistance R_r
1.73 GHz	42.39%	23.34 Ω
3.00 GHz	77.64%	35.46 Ω
4.23 GHz	65.87%	28.48 Ω

3.3.4 Comparison and Discussion

In rectangular shape the antenna operates at 3 GHz only (single band). Whereas, the S-shaped antenna works at three resonant frequencies 1.73 GHz, 3 GHz and 4.23 GHz (multiband). Designing S-shaped patch from rectangular one gave rise to two advantages:

- **Size reduction** with respect to the first frequency 1.73 GHz. Since, when trying to design rectangular patch operating at that frequency, the patch length and width would be of about 41.80 mm and 53.69 mm respectively. This leads to a surface reduction of about 68%.
- **Multiband operation** so that the antenna could be used for Radar applications and GSM applications as well.

3.4 Realization and Measurements

After analyzing and studying the simulated design with the IE3D software, a certain procedure is followed to implement and fabricate the physical structure of the design. A test is performed to validate the results.

3.4.1 Realization

The implementation of the desired antenna is done using the available PCB prototyping machine “MITS ELECTRONICS” shown in Figure 3.16 using the FR4 epoxy glass as a substrate material with a high precision cutter. The constructed antenna is shown in Figure 3.17.

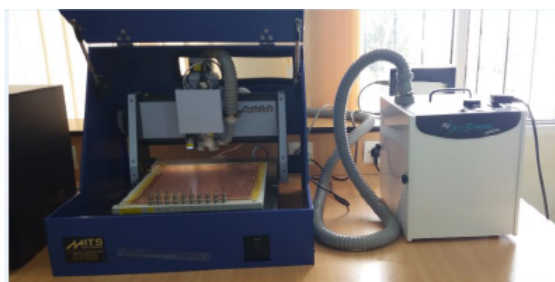


Figure 3.16: The PCB prototyping machine

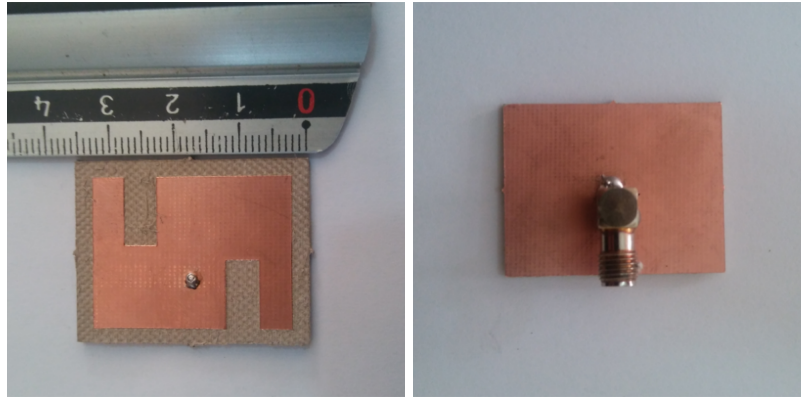


Figure 3.17: Rear and front view of the constructed S-shaped patch antenna

3.4.2 Measurements and Comparison

Using the vector network analyzer shown in Figure 3.18, the input reflection coefficient of the constructed antenna has been tested. For a clear image, the extracted data has been used to plot the measured input reflection coefficient with the simulated one using MATLAB (Appendix). Figure 3.19 shows its output.



Figure 3.18: The Vector Network Analyzer

Figure 3.19 indicates clearly that the designed antenna operates properly at the obtained frequencies. However some shifts between measurements and simulations are noticed; which may be attributed to the following factors:

1. The material used may have a relative dielectric constant different from 4.3;
2. The welding on the connector is done in inadequate manner;
3. The environment contains reflecting walls that may affect the input impedance of the antenna.

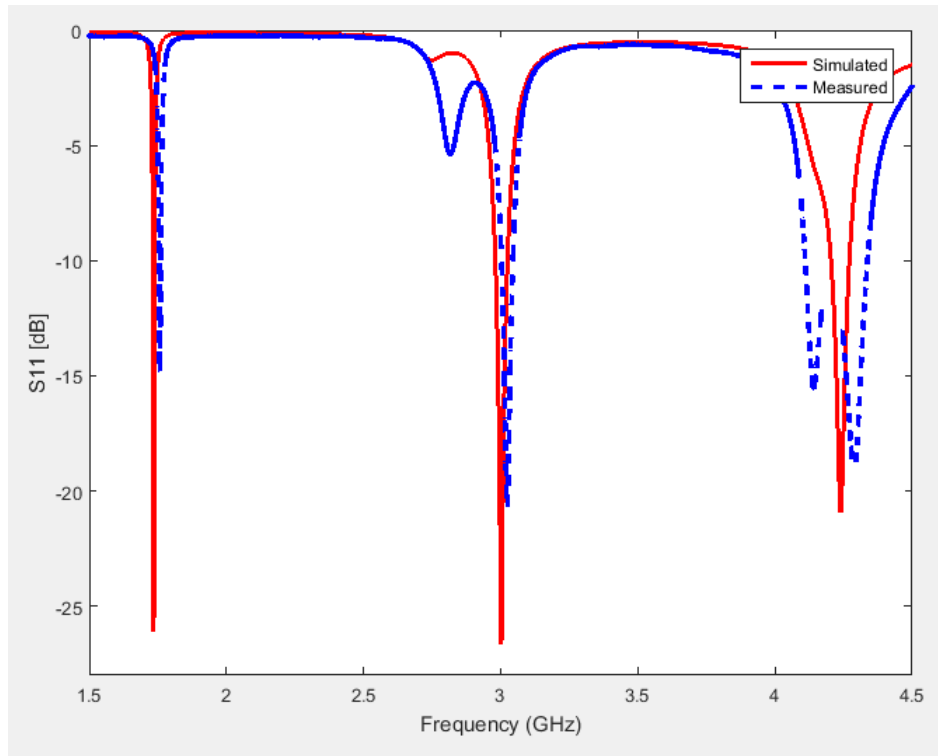


Figure 3.19: Measured and Simulated Input Reflection Coefficient of S-shaped patch antenna

The numerical results and the percentages of error in frequency, return loss and bandwidth are summarized in Table 3.6.

Table 3.6: Measured and Simulated characteristics of S-shaped Antenna with error percentages

Frequency GHz			Return Loss dB			Bandwidth %		
simulated	measured	error	simulated	measured	error	simulated	measured	error
1.73	1.75	1.15%	-26.11	-14.54	44.30%	0.35%	0.39%	0.11%
3.00	3.02	0.66%	-24.96	-20.43	18.14%	1.47%	1.35%	0.08%
4.23	4.29	1.41%	-20.91	-18.63	10.90%	1.65%	5.35%	2.24%

Conclusion

In this report, a new microstrip patch antenna having the S letter shape has been designed using IE3D simulator and fabricated by PCB "MITS electronics machine". The antenna operates at three bands including the desired frequency (3 GHz). The project successfully achieved its aim.

The work is initialized by designing a rectangular patch antenna working at the radar frequency (3 GHz) for purpose of familiarization with both the planar antennas as well the used software simulator. The RMSPA has been designed using transmission line method with coaxial probe feed, and simulated with some adjustments on the antenna size and the feed position towards improving the performance of the antenna. The obtained antenna characteristics match the expectations.

Then, the obtained RMSPA redesigned by cutting two rectangular slots with a view to get S-shaped patch. The extension of the analysis to the S-shaped antenna shows the possibility of multiband operation with the original frequency included. the resulted antenna could resonate at three frequencies 1.73 GHz which is suitable for GSM applications, 3 GHz for RADAR application, which is the desired frequency, and the second mode of the first frequency 4.23 GHz.

The S-shaped antenna has been implemented and tested by vector network analyzer, the measured reflection coefficient comparing to the simulated one was acceptable with a small shift of the frequencies. This shift may be attributed to realization precision as well as to the dielectric material which has a modified dielectric constant due the environmental conditions, since it is very old and is stocked for long time. Further more, there was shifts between the measured and simulated return loss values can be imputed to some impedance mismatches due to the coaxial microstrip transitions connector side.

Bibliography

- [1] Dustin M and Kyle S, (2016, Jun 02). "11 Myths About Antenna Design", Retrived from <http://www.electronicdesign.com/analog/11-myths-about-antenna-design>.
- [2] B. D. Patel: "Microstrip Patch Antennas - A Historical Perspective of the Development", Conference on *Advances in Communication and Control Systems* 2013 (CAC2S 2013), H. O. D, E. T Department, College Of Engineering Roorkee, Roorkee, U.A-247667, India
- [3] K.BOUTHIBA and N.BOUAMOCHA, *Design and Analysis of Y-Shaped Microstrip Antenna*, Master project, IGEE / UMBB, June 2017.
- [4] Constantine A. Balanis *ANTENNA THEORY ANALYSIS AND DESIGN - 3rd Edition*, John Wiley & Sons, Inc., Hoboken, New Jersey, 2005.
- [5] THOMAS A. MILLIGAN, *MODERN ANTENNA DESIGN-2nd Edition*, by John Wiley & Sons, Inc., Hoboken, New Jersey, 2005
- [6] Tapan Pattnayak, Guhapriyan Thanikachalam *Antenna Design and RF Layout Guidelines* Document No. 001-91445 Rev.
- [7] Pr. A. AZRAR, Lecture notes of *Antennas*, , Institute of Electrical and Electronics Engineering, University M'Hamed BOUGURRA Boumerdes, Algeria.
- [8] Ahmed F. Alsager, *Design and Analysis of Microstrip Patch Antenna Arrays*, Master thesis No. 1/2011, University College of Borås, School of Engineering 2011.
- [9] Prof. Sean Victor Hum, "Antenna Characteristics", Lecture notes of *ECE422: Radio and Microwave Wireless Systems*.
- [10] Mentor Graphics, formerly Zeland Software, Inc. (2010, August 3). "Datasheet: IE3D - Scalable EM Simulation Solution", Retrived from <https://www.rfglobalnet.com/doc/ie3d-scalable-em-simulation-solution-0001>.

Appendix

Code used for plotting comparison graph

The following figure shows the MATLAB code to plot the input reflection coefficient for both the measured and simulated results; these are plotted using the points recorded from the vector network analyzer and the points picked from simulation results respectively.

```
2 - clear all
3 - close all
4 - clc;
5
6 - % *****load the measurments Data*****
7 - load EXP20.txt;
8 - Data=EXP20;
9 - fm=Data(:,1)./10^9 % measures frequency vector
10 - s11m=10.*log(sqrt(Data(:,2).^2+Data(:,3).^2)); % measures S11 magnitude vector
11 - % measures S11 magnitude vector
12 - % *****load the simulation Data*****
13 - % *****load the measurments Data*****
14 - load test1.txt;
15 - Data=test1;
16 - fS=Data(:,1); % measures frequency vector
17 - s11S=Data(:,2); % measures S11 magnitude vector
18 - plot(fS,s11S,'r',fm,s11m,'b--','LineWidth',2,'MarkerSize',8)
19 - axis([1.5 4.5 -28 0])
20 - legend('Simulated','Measured')
21 - xlabel('Frequency (GHz)');
22 - ylabel('S11 [dB]');
```

Figure 3.20: MATLAB code to plot the input reflection coefficient for both the measured and simulated results